JAAS

Accepted Manuscript

This is an *Accepted Manuscript*, which has been through the Royal Society of Chemistry peer review process and has been accepted for publication.

Accepted Manuscripts are published online shortly after acceptance, before technical editing, formatting and proof reading. Using this free service, authors can make their results available to the community, in citable form, before we publish the edited article. We will replace this *Accepted Manuscript* with the edited and formatted *Advance Article* as soon as it is available.

You can find more information about *Accepted Manuscripts* in the Information for Authors.

Please note that technical editing may introduce minor changes to the text and/or graphics, which may alter content. The journal's standard Terms & Conditions and the Ethical guidelines still apply. In no event shall the Royal Society of Chemistry be held responsible for any errors or omissions in this *Accepted Manuscript* or any consequences arising from the use of any information it contains.

ROYAL SOCIETY OF CHEMISTRY

www.rsc.org/jaas

Neodymium isotope ratio measurements by LC-MC-ICPMS for nuclear applications: investigation of isotopic fractionation and mass bias correction.

Florence Guéguen[1], Hélène Isnard[*1], Anthony Nonell[1], Laurent Vio[1], Thomas Vercouter[1], Frédéric Chartier[2]

1. Commissariat à l'Energie Atomique et aux Energies Alternatives (CEA), DEN, DPC, SEARS, LANIE, F-91191 Gif Sur Yvette, France

2. Commissariat à l'Energie Atomique et aux Energies Alternatives (CEA), DEN, DPC, F-91191 Gif Sur Yvette, France

* Corresponding Author: Hélène Isnard, helene.isnard@cea.fr

Abstract (50-250 mots)

Accurate measurements of neodymium isotope ratios in irradiated nuclear fuel samples are fundamental for the validation of neutronic calculation codes, in particular for burn-up qualification. To prevent possible spectral and non-spectral interferences, neodymium is generally purified from the complex sample matrices prior to measurements by mass spectrometric techniques. This work describes the on-line coupling of ion exchange chromatography with a multi-collector inductively coupled plasma mass spectrometer for Nd isotope ratio measurements. In the first part of the paper, the causes of the isotope ratio drifts traditionally observed during transient signal acquisitions are investigated. Both mass-dependent isotopic fractionation on the chromatographic column and distinct time lags between amplifier responses of the Faraday cup configuration were shown to be the main phenomena involved in the observed isotope ratio drifts. In the second part, we present a new approach for mass bias correction called "Intra Injection Sample-Standard Bracketing (IISSB)" based on direct "on-line" injection of the standard via the chromatographic system before and after the analyte. This new method, particularly adapted to analysis of nuclear materials, was validated by on-line measurements on a simulated sample representative of fission products present in an irradiated uranium material. Reproducibilities obtained by IISSB were found to be comparable with those found in off-line measurements and classical sample-standard bracketing technique for mass bias correction on all Nd isotope ratios.

Keywords: Nd isotope ratios, isotopic fractionation, mass bias correction, LC-MC-ICPMS, transient signal

1. Introduction

In the nuclear research field, the precise knowledge of the isotopic composition of actinides and fission products and their atomic ratios with respect to uranium is mandatory to improve the nuclear fuel management and neutronic calculation code qualification. The main requirement is to obtain the best accuracy of elemental and isotope ratio determination. Mass spectrometry techniques involving multiple collector systems such as thermal ionization mass spectrometry (TIMS) and multiple collector inductively coupled plasma mass spectrometry (MC-ICPMS) have the capability of very accurately measuring isotope ratios. These mass spectrometric measurements are generally subsequent to a chromatographic elemental separation procedure[1-4] to prevent possible spectral (isobaric, polyatomic or doubly charged) and non-spectral (matrix effects) interferences on the element of interest.

Nd is one of the fission products present in nuclear fuel samples or irradiated uranium and/or plutonium materials and is a precise burn-up indicator (degree of fuel consumption)[5-7]. Therefore, Nd isotope ratios (all Nd isotopes are of interest in the nuclear field for various purposes) are determined routinely in nuclear fuel samples or irradiated actinide materials[8, 9]. In our laboratory, Nd is usually isolated from the complex nuclear sample matrix using a two-step chromatographic separation procedure [3, 10]. The first step leads to the chemical purification by gravitational chromatography of U and Pu from the sample. The second step aims at individual isolation by High Performance Liquid Chromatography (HPLC) of Nd and other analytes of interest from the complex residual Fission Products/Minor Actinides fraction (FP fraction).

On-line coupling of liquid chromatography to an inductively coupled plasma mass spectrometer (ICP-MS) is a well-established method to reduce the handling time and consequently the analyst's exposure to radiation in the case of radioactive samples. Several

applications of coupling between ion chromatography (IC) and quadrupole inductively coupled plasma mass spectrometry (Q-ICPMS) for lanthanides are reported in the literature[1, 11-14]. To obtain accurate measurements of Nd isotope ratios, the coupling between IC and multiple collector inductively coupled plasma mass spectrometry (MC-ICPMS) is one of the most attractive approaches for nuclear[15] and geochemical applications[16]. However, the acquisition of transient signals has been found to be challenging compared with continuous ones. A drift of the isotope ratios is classically observed during transient signal acquisition as well as a significant decrease of the external precision of isotope ratios [17-23]. The origins of this drift is a matter of debate, and both instrumentation and/or separation devices (HPLC, and gas chromatography (GC)) can be involved depending on the configuration. In addition, internal normalization for mass bias correction cannot be applied on nuclear samples because no invariant ratios are available[15, 24]. Therefore, bracketing procedures with successive injections of standard – sample – standard in HPLC/MC-ICPMS coupling are often applied for this purpose[15, 18].

In this study, the performances of an LC-MC-ICPMS coupling were tested in the case of Nd isotope ratio measurements in simulated fission product fraction from a ^{235}U irradiated target. In a first step, the possible causes of the isotope ratio drift observed during transient signal acquisition at our particular instrumental settings were investigated. We then present a new approach called Intra Injection Sample-Standard Bracketing (IISSB) for mass bias correction based on the injection of a reference standard before and after the Nd elution peak. The reproducibility obtained on the Nd isotope ratio measurements using different methods of data treatment[25, 26] is discussed.

2. Materials and methods

2.1. Reference materials and reagents

Isotopic reference material. For Nd isotopic measurements, the *JNdi-1* standard solution was used[27]. This material is qualified for its $^{143}Nd/^{144}Nd$ isotope ratio and is especially employed in geochemical applications. In irradiated materials, all Nd isotope ratios have to be measured. Reference values of isotope ratios are generally qualified by TIMS using the total evaporation method[28, 29]. In this study, we used the *JNdi-1* values obtained by Wakaki et al.[29] and using the normalization ratio $^{146}Nd/^{144}Nd = 0.72333$ defined by the total evaporation method[28]. These reference values, used for mass bias correction in the present study, are listed in Table 1.

Elemental solutions. Solutions were prepared daily by appropriate dilution of the 10^3 $\mu g \cdot mL^{-1}$ individual stock standard solutions of Mo, Ru, Gd, Eu, Sm, Cs, Nd, Pr, Ce, La and Sr (from Specpure®, Schiltigheim, France). All sample dilutions were performed with 0.5M HNO_3 obtained from 65% ultra-pure nitric acid (Suprapur from Merck, Darmstadt, Germany) and de-ionized water (Milli-Q system, Millipore, Milford, USA). The chromatographic eluent for lanthanide separation was prepared daily by dissolution of 2-hydroxy-2-methylbutyric acid HMB (Sigma–Aldrich, Saint-Quentin-Fallavier, France) in purified water. The pH of the mobile phase was adjusted with a 25% ammonia solution (Merck, Darmstadt, Germany).

2.2.Instrumentation

2.2.1. High Performance Liquid Chromatography (HPLC)

The lanthanide separation was performed with a chromatographic system composed of a binary analytical pump (ICS 5000 Dionex) combined with an analytical column, LUNA SCX

and a guard column (Phenomenex, Torrance, CA, USA). The column diameter was 4.6 mm and different column lengths were used (250, 150, 50 mm). The stationary phase consisted of silica bonded with benzene sulfonic acid groups from the same batch. The particle size was 5 µm. All tubings were in polyetheretherketone (PEEK). The samples were injected using a six-way Rheodyne valve. All parameters of the chromatographic system and the separation conditions are listed in Table 2.

2.2.2. MC-ICPMS

Nd isotope ratios were determined on a *NEPTUNE Plus* MC-ICPMS (Thermo Scientific, Bremen, Germany), modified in order to accommodate a glove box around the ion source. Operating parameters are detailed in Table 2. The analyses were conducted at low mass resolution and in static mode. Faraday cups were positioned in order to simultaneously measure the seven Nd isotopes and to correct for potential Ce and Sm isobaric interferences by monitoring ^{140}Ce and ^{147}Sm (Table 2).

Continuous mode. A stable introduction system (SIS) composed of a 100 µl.min^{-1} microconcentric PFA nebulizer (Elemental Scientific, ESI, USA) mounted onto a tandem quartz spray chamber arrangement (cyclonic + Scott double pass) was used. The sensitivity was optimized on a daily basis for maximum intensity and stability. In SIS mode, the sensitivity was around 70V/ppm for Nd during the analytical sessions and the Nd acquisition method consisted of 50 integrations (5 blocks of 10 cycles) with an integration time of 8.4s, and removal of outliers using a 2σ test. Further data treatment was performed off line. The instrumental mass fractionation (mass bias) was corrected by classical Sample Standard Bracketing (SSB) using an exponential fractionation law[30]. Concentrations of samples and bracketing standards were matched to within 20%. The results and reproducibility obtained on the *JNdi-1* standard with this approach during the analytical sessions are presented in Table 1.

Hyphenated mode. To adapt the flow rate between the chromatographic column and the ICPMS, the column output tubing was split using a "Y" connection. Only 10% of the flow was sent to the MC-ICPMS via a 100 µL.min^{-1} pneumatic glass concentric nebulizer (Meinhard Glass Product, Golden, USA). (Figure 1A). For transient signals, the acquisition time was set at 0.262s (discussed later).

For isotope ratio drift investigations on transient signals, some experiments were performed by flow injection analysis (FIA). In this case, a six-way Rheodyne valve was directly coupled to the nebulizer of the MC-ICPMS.

For the implementation of the IISSB approach for mass bias correction, a particular instrumental setting called "dual inlet LC-MC-ICPMS" was developed (Fig. 1B). This system rendered it possible to inject the reference standard at a 1 mL.min^{-1} flow rate using a second chromatographic pump, at selected steps of the elution (before and after Nd elution peak). In this case, a second six-way Rheodyne valve was used and the split ratio was modified in order to send only 5% of the flow to the ICP. As for the continuous mode, both sample and bracketing standard concentrations were matched to within 20%.

2.2.3. Q-ICPMS

A quadrupole inductively coupled plasma mass spectrometer X series II (Thermo Electron, Winsford, UK) was used for elemental determinations. Sample introduction was performed with a pneumatic quartz concentric nebulizer (0.4 ml.min^{-1}) connected to a quartz cyclonic spray chamber and using a PC^3 Peltier Chiller (Elemental Scientific, ESI, USA). The instrument was optimized daily with a 1 ng.g^{-1} multi-element test solution in order to obtain the maximum counting rates and stability on ^{115}In and ^{238}U signals. The key parameters (sensitivity, stability, and oxide level) were verified daily. The employed Q-ICPMS instrumental parameters are summarized in Table 2.

3. Results and discussion

3.1. Drift phenomenon investigations

Previous studies performed when coupling LC and MC-ICPMS have shown isotope ratio drift during acquisition on transient signals (see [22] and reference therein). This phenomenon largely detailed in the literature is generally ascribed to a variety of sources (such as mostly variable time responses between Faraday amplifiers[31], isotope fractionation during separation[32], …) without an assessment of their individual contribution.

First, the acquisition of Nd isotope ratios on transient signals with our coupling was studied. A single elemental solution of *JNdi-1* was injected in the chromatographic column (length 250 mm) at a concentration of 50 $\mu g.g^{-1}$ which corresponds to an injected mass of 500 ng (injection volume of 10 µl). Considering the split conditions, about 50 ng of Nd was sent to the ICPMS (Figure 1A). The maximum intensity collected on the ^{142}Nd isotope was 30 volts. Considering that the maximum signals collected were higher than 5 volts at the peak apex for all isotopes, baseline contributions were negligible, and a 10 mV signal threshold on the ^{142}Nd isotope was chosen for the beginning of the data treatment (baseline of the ^{142}Nd isotope was around 0.5 mV before the elution peak).

The integration time was set at 0.262 s corresponding to roughly 400 data points for each elution peak. Different integration times (0.008 s to 1.049 s) were tested with no effect on the amplitude of the drift. Figure 2 displays the $^{143}Nd/^{144}Nd$ isotope ratio and ^{144}Nd signal as a function of the elution time. A significant drift phenomenon was observed for the $^{143}Nd/^{144}Nd$ ratio along the elution peak. The amplitude of the drift for this ratio was graphically estimated to about 4.2‰ per amu. This drift amplitude of the isotope ratio was also evaluated for the

other Nd isotope ratios and was found to vary from 1.4‰ to 8.9‰ (Supplementary information (SI), Figure S1) with no mass dependency observed. Investigations performed to understand the dominant sources of these variations are described below.

3.1.1. Isotope fractionation on the chromatographic column

Previous studies have revealed that the chromatographic separation technique can be a source of isotope fractionation of Nd isotopes during elution. On gravitational cationic exchange resin (BioRad AG 50WX8) and when using HIBA as a complexing agent, an amplitude of isotope fractionations around 0.7‰ per amu was observed[29]. Another study[33] has demonstrated a slight Nd isotope fractionation (<0.1‰ per amu) using a combination of TRU and Ln Spec (Eichrom) resins with HNO_3 as the eluent. Furthermore, it is well documented that band displacement chromatography is an efficient process to obtain enriched isotopes. There are also reports of the separation of Ce, Nd and Gd isotopes using various cationic exchange resins at several migration lengths and using different eluents[34-39].

The possible extent of Nd isotope fractionation in the chromatographic system was then evaluated. A drop-wise Nd fraction recovery was performed along the elution peak in order to constrain only the drift phenomenon induced by the separation. Experiments were carried out using different column lengths (250 mm, 150 mm and 50 mm) with the same diameter (4.6 mm) and the same batch of stationary phase. The flow rate was the same for the three columns (1 $ml.min^{-1}$).

For these experiments, five µg of the *JNdi-1* solution were injected in the chromatographic columns using the setup presented in Figure 1A. Drop-by-drop recovery was performed along the Nd chromatographic peak. Depending on column lengths (250, 150 and 50 mm) 13, 14 and 23 drops were respectively recovered. Each drop was evaporated dry before dilution in

HNO_3 0.5M in order to prevent from potential matrix effect due to organic acid. Each solution was characterized for its Nd concentration in a semi-quantitative way (~20% uncertainty) by Q-ICPMS. One µl of solution was diluted in HNO_3 0.5M and analyzed by Q-ICPMS by external calibration using an Nd Spex single element standard solution. Each solution was also adjusted in concentration to 50 $ng.g^{-1}$ and Nd isotope ratios were performed by SIS-MC-ICPMS on the Neptune Plus MC-ICPMS. The instrumental mass bias was corrected using classical Sample-Standard Bracketing (SSB) with the *JNdi-1* reference standard solution.

The results for mass concentration and $^{143}Nd/^{144}Nd$ and $^{148}Nd/^{144}Nd$ isotope ratios obtained for each drop on the 250-mm chromatographic column are presented in Figure 3. The $^{143}Nd/^{144}Nd$ ratio variation from lower values at the early stage of elution to higher values at the late stage corresponding to a variation of around 2.4‰ per amu indicate a preferential elution of heavy isotopes. Conversely, the $^{148}Nd/^{144}Nd$ ratios varied from higher to lower values corresponding to a similar variation of around 2.4‰ per amu suggesting a mass-dependent isotopic fractionation confirmed in the three-isotope plots (Figure 4).

Three independent injections and drop recuperations were performed and the uncertainty on the amplitude variation per amu was estimated to be 0.2 ‰. The $^{143}Nd/^{144}Nd$ isotope ratio calculated by mass balance between the 13 drops corresponded to a value of 0.51161 (uncertainty not evaluated) in agreement with reference value[29], demonstrating a complete Nd recovery.

Beta values for experimental, equilibrium and kinetic laws[40] were evaluated and no clear conclusions could be drawn relative to the isotope fractionation mechanisms. For the shorter columns (150 mm and 50 mm), the amplitude of fractionation was evaluated at 1.8‰ and 1.4‰ on the $^{143}Nd/^{144}Nd$ ratio, respectively. As mass dependent isotope fractionation was confirmed in all three isotope plot diagrams, this indicated that mass fractionation was

dependent on the length of the column. The amplitudes of fractionation observed were larger than those observed on gravitational ion-exchange chromatography[29, 33]. This high amplitude might be linked to the higher number of theoretical plates involved in our HPLC column (about 1000 times higher than in typical gravitational chromatography).

These experiments clearly revealed that mass-dependent isotopic fractionation, with elution of heavier isotopes earlier than the lighter, can be considered as a significant source of isotope ratio drifts during transient signal acquisition in our system. However, as the final observed drifts (Figure S1) were not purely mass-dependent, other potential drift sources were investigated.

3.1.2. Delay lag of Faraday cup amplifiers

Among the other potential sources of isotope ratio drift is the slow and variable time response of the amplifier system of the Faraday cups against changes of the input ion signal. A recent study[31] has demonstrated that during transient acquisition the slight time lags between amplifiers involved in the Faraday detector array were able to generate significant isotope ratio drifts. This demonstration was based on experiments performed by flow injection connected to a demountable direct injection high efficiency nebulizer (d-DIHEN) on a Neptune MC-ICPMS.

The Neptune MC-ICPMS offers the possibility of virtually assigning any amplifiers to any Faraday cups. Therefore, some experiments were performed with the Neptune Plus instrument by switching the amplifiers on the same couple of Faraday cups for different injections. The results are presented in Figure 5. For these experiments, the *JNdi-1* standard was injected in the chromatographic column (250 mm) and ^{143}Nd and ^{144}Nd signals were collected on L2 and L1 Faraday cups. In Figure 5A, L2 and L1 were assigned to amplifiers OA2 and OA4 respectively and a drift amplitude of about 4.9‰ was observed with a positive slope. For the

next injection, OA2 and OA4 were switched between L2 and L1 and an inversed drift slope (negative slope) with significantly lower amplitude was seen (Figure 5C). In Figure 5E, OA4 was replaced by OA3 on the L1 Faraday cup and the amplitude of the observed drift was then around 2.2‰ (again with a positive slope). This indicates that the amplitude of the drift was dependent on the amplifiers used. These experiments clearly confirm that individual amplifier time lags have a significant impact on the observed drifts.

To estimate the time lags between the three amplifiers used, Nd was injected by flow injection (the rheodyne injection valve was directly connected to the nebulizer of the MC-ICPMS) in order to suppress the contribution of the drift due to column fractionation. The results are presented in Figure 5B, D and F. Figure 5B shows the ^{143}Nd and ^{144}Nd signals respectively acquired with L2 and L1 Faraday cups with OA2 and OA4 amplifiers. In this configuration, the ^{144}Nd signal was acquired in advance relative to ^{143}Nd. This suggests that the OA4 amplifier had a faster response than the OA2 amplifier in our instrument. When switching these two amplifiers between L2 and L1, reverse drift was observed (Figure 5D). Using the Exponential Modified Gaussian model (EMG)[41], the elution profile of each isotope was fitted in order to precisely assess the elution time at their peak apex. The slight differences between each elution time at the maximum of the isotope peaks were directly related to the time lags between the amplifiers. For OA2 and OA4, this delay was about 5 ms. Likewise, using OA2 and OA3 amplifiers on L2 and L1 faraday cups (Figure 5F), the drift was reduced and the time lag between OA2 and OA3 was estimated to 0.5 ms. These observations confirmed the range of time lag previously observed by direct injection on another Neptune MC-ICPMS instrument[31]. According to future technological developments, this phenomenon might be reduced in the future.

The first part of this paper has demonstrated that both mass-dependent column fractionation and time lags between amplifiers can explain in our setting the magnitude and the non-mass

dependent drifts observed during our LC-MC-ICPMS experiments (Figure S1). Investigations on data treatment (peak area integration[25] or linear slope regression methods[26]) to compensate these drifts as well as instrumental mass bias corrections methods are presented in the next part.

3.2. Results on Nd ratio measurements by LC-MC-ICPMS

Experiments were performed on a simulated sample representative of the fission products fraction present in a ^{235}U transmutation target irradiated in a French nuclear reactor[42, 43]. These experiments required accurate Nd isotope ratios for use of fission monitors[44, 45]. A mass spectra obtained by Q-ICPMS in the m/z= 80-160 mass range on the real FP fraction in the ^{235}U target is presented in supplementary information (Figure S2). Conventionally in the laboratory, Nd isotope ratios are determined after separation (of the FP fraction) by HPLC on a LUNA SCX column[46] and Nd fractions are collected and analyzed off line by TIMS or MC-ICPMS. The uncertainties targeted for such analyses are around 0.2% for all isotope ratios[10]. A simulated solution containing lanthanides and metallic elements present in the fission product fraction (Sr, Mo, Ru, Cs, La, Ce, Pr, Nd, Sm, Eu and Gd) and in the same mass proportion as those found in the irradiated ^{235}U target was prepared.

3.2.1. Chromatographic conditions

The elution conditions have been adjusted, especially the gradient slope, in order to reduce the analytical time while presenting a resolution of at least 2 between Nd and its neighboring peaks (Sm and Ce). In FP fractions, Sm interferes with Nd at masses 148 and 150 and Ce interferes with Nd at masses 142 and 144. A resolution of two means that peak overlapping was lower than 0.05%. The linear gradient started at the time of the injection (t=0 min, 100% of HMB 0.1M, pH=3.6) and at the end of the program (t=35 min) there was 100% of the second eluent (HMB 0.2M, pH=4.5). The separation obtained under these conditions and

using a Q-ICPMS as the detector is presented in Figure 7. The 11 elements were separated in the following elution order: Mo, Ru, Gd, Eu, Sm, Cs, Nd, Pr, Ce, La and Sr. Nd was eluted after 15 minutes and was separated from its potential interferents Sm ($t_{elution}$= 11 minutes) and Ce ($t_{elution}$=20 minutes). As shown in Figure 6, the Nd elution peak was included in the decreasing part of the Cs peak with no consequence as Nd and Cs isotopes do not interfere.

3.2.2. Mass bias correction approach

Since there is no invariant ratio usable for Nd in an irradiated sample, the internal mass bias correction traditionally performed in geochemical applications[47] cannot be applied to nuclear samples[15, 18, 24]. In the nuclear field, the most conventional approach is the SSB. To compensate for the matrix effect previously observed in the literature[18], the reference standard has to be injected via the LC system in the same conditions as the sample[48]. In addition for optimal performance this approach requires a short analysis time between the sample and the two standards.

To optimize both bracketing standard injections and gradient matching, a new approach called Intra Injection Sample-Standard Bracketing (IISSB) was developed. For this purpose, a rheodyne valve controlled by a second chromatographic pump was added in order to inject the standards during the elution (Figure 1B). The chromatographic system was set to guarantee a perfect matrix matching between the separation flow (branch (a), Figure 1B) and the standard flow (branch (b), Figure 1B). The start of the gradient in branch (b) was delayed for a period of time corresponding to the difference in void volume between branch (a) and (b). By this way, at the converging point of the two flows, the matrices were rigorously similar.

Some experiments were performed by injecting only the standard by branch (b) and no significant variations of mass bias were observed regardless of the HMB concentration during the elution gradient. To define the appropriate timing for injecting the Nd bracketing

standards before and after Nd elution peak (of the sample), baselines on Nd isotope signals were carefully controlled. For the injection of the first standard, in order to minimize the baseline contribution, it was essential that the Sm signals, that could interfere with the Nd isotopes (^{144}Sm, ^{148}Sm, ^{150}Sm), had returned to the baseline values < 1mV. Following this, the first Nd standard could be injected 1 minute after the Sm peak or 4 minutes before the Nd peak sample (figure 7B). For the second injection, as there was not enough time for an injection between Nd and Ce (isobaric interferences at masses 142 and 144 in nuclear fuel samples), the Nd standard was thus injected just after the La peak (7 minutes after the Nd peak).

3.2.3. Reproducibility on Nd isotope ratios

Different methods of data treatment can traditionally be used for the determination of raw isotope ratios on transient signals. Among these, the point by point (PbP), linear regression slope (LRS) and peak area integration (PAI)[22, 25, 26, 49] techniques have been intensively compared in literature[22]. The LRS and PAI methods are used for transient signals because they correct the isotope ratio drifts[25, 26]. In the PbP and PAI methods, the background is taken into account by subtracting the baseline before the elution of the peak. In our case, the baseline corrections were negligible. In this work, the PbP and PAI calculation methods were applied for the different zones of the peak, similarly to the approach previously described[49]. Considering the reproducibility and accuracy obtained at different zones of the peak, an integration window of 95% was chosen for the PbP and PAI approaches. As the LRS method does not require the selection of a specific percentage of the peak area[26], 100% of the peak zone was considered.

Table 3 presents the results obtained on six injections of a ^{235}U simulated fraction containing simulated Nd Spex solution (concentration of 500 $ng.g^{-1}$) on the chromatographic column. Mass bias was corrected with the IISBB approach for all ratios using the *JNdi-1* solution. Data on the bracketing standard and simulated sample were evaluated using the same data treatment technique. The last column of the table lists the $^{143}Nd/^{144}Nd$ ratio as calculated by internal mass bias correction using the $^{146}Nd/^{144}Nd$ ratio in order to carry out a comparison with data obtained in previous studies[16].

The results were compared with those obtained on the Nd Spex solution analyzed at a concentration of 50 $ng.g^{-1}$ on continuous signals corrected for mass bias by a classical SSB approach. The isotope composition of the Nd Spex solution was different of the *JNdi-1* isotopic standard composition in agreement with a previous study[29]. According to Table 3, all of the isotope ratios obtained by on-line measurements were in agreement with isotope ratios measured off-line and no bias was observed. The LRS and PAI methods gave a better external reproducibility than the PbP method. These results were in agreement with a previous investigation[25]. The best reproducibilities were obtained with LRS and were comparable to those acquired by the off-line procedures. The interest of the IISSB approach using LRS method of data treatment was demonstrated for application in the nuclear field.

Considering the $^{143}Nd/^{144}Nd$ ratio internally corrected for mass bias, the best reproducibility was found using the LRS method and this reproducibility was only slightly larger than counterparts obtained in continuous mode by a factor below two, which is in agreement with previous Nd isotope ratios obtained in transient mode[16].

Conclusion

The present article has described the coupling between a LUNA SCX chromatographic column and a MC-ICPMS Neptune Plus for lanthanide separation and on-line Nd isotope ratio measurements on nuclear samples. The first part of the study was dedicated to the comprehension of isotope ratio drifts observed during transient signal acquisition with our particular instrumental settings. In our chromatographic system, Nd isotope ratio variation due to column fractionation was evaluated by collecting the column outlet of several Nd peak fractions and analyses in continuous sample introduction mode. For the 250-mm column, 2.4 ± 0.2 ‰ per amu of isotopic drift was explained by isotopic fractionation on the column. Subsequent tests performed by virtually assigning any amplifiers to any Faraday cups confirmed that another contribution of isotope ratio drift was attributed to the different time lags between amplifiers. Moreover, the amplitude of the drift was dependent on the amplifiers used on each Faraday cup. Both mass-dependent column fractionation and the time lag between amplifiers can mostly explain in our setting the magnitude and the non-mass dependent drifts observed during our LC-MC-ICPMS experiments.

In a second part of the study, a new method for mass bias correction called Intra Injection Sample-Standard Bracketing (IISSB), based on the injection of an Nd reference standard before and after the Nd elution peak, was proposed. The reproducibility obtained on all Nd isotope ratios on a simulated ^{235}U FP fraction, using linear regression slope (LRS) and peak area integration (PAI) methods of data treatment, was lower than 0.2% and comparable to isotope ratio uncertainties obtained by an off-line procedure and Sample Standard Bracketing (SSB) mass bias correction.

The feasibility and performances on such on-line Nd isotope ratio measurements have been demonstrated as an alternative to off-line methods for nuclear samples. Further studies are required to strengthen the performances of this procedure for applications on real samples. This method is particularly attractive for reducing the analysis time and consequently the

analyst's exposure to radiation. Further developments are also required to reduce the waste volumes of effluent by decreasing the flow rate of the chromatographic system (chromatographic column and standard injection). An automation of the system may also be envisaged as an optimization.

Table 1: Nd isotope ratios of *JNdi-1*[29] and Nd isotope ratios obtained in continuous introduction mode and using the SSB method on the *JNdi-1* standard. * $^{146}Nd/^{144}Nd$ value of Dubois et al[28]. These values are in agreement with Nd data on the *JNdi-1* acquired by TIMS using the total evaporation method in our laboratory[50].

Table 2: Parameters of the liquid chromatography and operating conditions for the ICPMS instrumentation.

Table 3: Results of Nd isotope ratios on an Nd Spex solution. Off-line data were obtained on an Nd Spex solution and mass bias was corrected using an SSB approach. On-line data were obtained on an Nd Spex doped with other elements (Sr, Mo, Ru, Cs, La, Ce, Pr, Sm, Eu and Gd) and different methods of data treatment (peak area integration, linear slope regression and point by point). Mass bias was corrected with the IISSB method using a *JNdi-1* solution. * $^{143}Nd/^{144}Nd$ isotope ratio internally corrected using the value $^{146}Nd/^{144}Nd = 0.72333$[28]. The uncertainties represents the standard deviation of the n measurements expressed at k=2.

Figure 1: Schematic diagrams of (a) the LC-MC-ICPMS system and (b) the dual inlet LC-MC-ICPMS system with post-column addition of standard to perform intra injection mass bias correction.

Figure 2: Elution profile of the ^{144}Nd signal (*JNdi-1* standard solution) by LC-MC-ICPMS in gradient mode (integration time 0.262 s) and uncorrected $^{143}Nd/^{144}Nd$ isotope ratios across the transient signals. The approximate amplitude of the drift was estimated by the variation of isotope ratios between the two horizontal lines.

Figure 3: Nd concentration profile and $^{143}Nd/^{144}Nd$ and $^{148}Nd/^{144}Nd$ isotope ratios in the eluted drops after chromatographic separation on the LUNA SCX column (l=250 mm). The error bars for mass concentration correspond to a relative standard deviation equal to 20%. The error bars for isotope ratio correspond to a relative standard deviation at k=2 of three

replicate analyses. The dotted lines represent the $^{143}Nd/^{144}Nd$ and $^{148}Nd/^{144}Nd$ reference values[29].

Figure 4: Three isotope plots of Nd isotope ratios using the approach developed by Young et al[40]. The experimental mass-dependent fractionation of the $^{14X}Nd/^{144}Nd$ and $^{146}Nd/^{144}Nd$ was a straight line. The slope of the linear regression line was equal to the fractionation exponent β. The uncertainty associated with the Nd isotope ratios was smaller than the data points.

Figure 5: Uncorrected $^{143}Nd/^{144}Nd$ isotope ratio across the transient signals by LC-MC-ICPMS (A, C, E) and FIA (B, D, F). Different amplifiers were successively attributed to Faraday cups: configuration A and B: ^{143}Nd: OA2; ^{144}Nd OA 4; configuration C and D: ^{143}Nd: OA 4; ^{144}Nd OA 2; configuration E and F: ^{143}Nd: OA2; ^{144}Nd OA 3.

Figure 6: A: Chromatographic separation of a representative fission product fraction of a ^{235}U-irradiated target with a LUNA SCX column (Ø 4.6 mm) at a flow rate of $1ml.min^{-1}$ and T=20°C. The elution gradient started at t=0 min with 100% HMB at 0.1M in water, pH=3.6 and finished at t=35min with 100% HMB at 0.2M in water, pH=4.5. B: ^{143}Nd intensity signal recorded by MC-ICPMS during the time of elution. The Nd standard was injected between the Sm and Nd peaks ($t_{elution}$=720s) and after the La peak ($t_{elution}$=1450s).

Figure S1: Elution profile of the ^{144}Nd signal (*JNdi-1* standard solution) by LC-MC-ICPMS in gradient mode (integration time 0.262 s) and uncorrected $^{14x}Nd/^{144}Nd$ isotope ratios across the transient signals. The approximate amplitude of the drift was estimated by the variation of isotope ratios between the two horizontal lines.

Figure S2: Mass spectrum by Q-ICP-MS of the ^{235}U target sample between 80 and 160 amu. Mo is a fission product element but its presence was essentially due to the 2% of Mo present in the steel container incorporating the ^{235}U target.

Sample	$^{142}Nd/^{144}Nd$	$^{143}Nd/^{144}Nd$	$^{145}Nd/^{144}Nd$	$^{146}Nd/^{144}Nd$	$^{148}Nd/^{144}Nd$	$^{150}Nd/^{144}Nd$
JNdi-1 **(internally normalized to** $^{146Nd}/^{144Nd}$**=0.72333*)**	1.13957(3)	0.511592(5)	0.348757(2)	0.72333	0.242538(3)	0.237853(10)
JNdi-1 **MC-ICPMS measurements by SSB (n=16)**	1.13957(10)	0.511591(29)	0.348757(17)	0.72333(6)	0.242539(31)	0.237855(48)

Table 1

Liquid chromatography parameters

HPLC pump	Binary analytical pump ICS 5000 Dionex
column	LUNA SCX (Strong Cation Exchange) (250 mm × 4.6 mm)
	guard column
eluent	2-hydroxy-2-methylbutyric acid HMB 0.1M pH 3.6 (*Eluent A*)
	HMB 0.2M pH 4.5 (*Eluent B*)
flow rate	1 $mL.min^{-1}$
gradient elution	
t=0min	100% A; 0% B
ramp between 0-35min	
t=35min	0% A; 100% B

Neptune Plus MC-ICPMS operating conditions

RF power	1100 W
Plasma gas flow rate	15.0 $L.min^{-1}$
Auxiliary gas flow rate	1.0 $L.min^{-1}$
Nebulizer gas flow rate	0.95 $L.min^{-1}$
Sample uptake rate	0.1 $mL.min^{-1}$
Nebulizer type	100µ$L.min^{-1}$ PFA nebulizer (ESI) (continuous mode)
	100µ$L.min^{-1}$ pneumatic glass concentric nebulizer (hyphenated mode)
Spray chamber type	quartz dual spray chamber (cyclonic + double pass)
Acquisition method	
continuous mode	5 blocks, 10 cycles, 8.4s integration
transient mode	1 block, between 700 and 5000 cycles, 0.262s integration

Faraday Cup Configuration

Cups	**L4**	**L3**	**L2**	**L1**	**Ax**	**H1**	**H2**	**H3**	**H4**
Mass	140	142	143	144	145	146	147	148	150

ICP-Q-MS operating conditions

RF power	1100 W
Plasma gas flow rate	15 $L.min^{-1}$
Auxiliary gas flow rate	1.0 $L.min^{-1}$
Nebulizer gas flow rate	0.9$L.min^{-1}$
Sample uptake rate	0.2 $mL{\cdot}min^{-1}$
Nebulizer type	400 µ$L.min^{-1}$ pneumatic glass concentric nebulizer
Spray chamber type	PC^3 Peltier Chiller with a cyclonic spray chamber

Table 2

	$^{142}Nd/^{144}Nd$	$^{143}Nd/^{144}Nd$	$^{145}Nd/^{144}Nd$	$^{146}Nd/^{144}Nd$	$^{148}Nd/^{144}Nd$	$^{150}Nd/^{144}Nd$	$^{143}Nd/^{144}Nd$*
Off line			**Standard bracketing with *JNdi-1***				
Average (n=8)	1.13997 (14)	0.51127 (3)	0.34870 (3)	0.72309 (9)	0.24238 (6)	0.23762 (8)	0.511206 (14)
On line			**Standard bracketing, data treatment: peak area integration PAI (95%)**				
Average (n=6)	1.13986 (15)	0.51130 (3)	0.34871 (4)	0.72311 (14)	0.24224 (13)	0.23754 (9)	0.511177 (23)
			Standard bracketing, data treatment: linear regression slope LRS (100%)				
Average (n=6)	1.13992 (17)	0.51129 (4)	0.34871 (3)	0.72312 (8)	0.24229 (3)	0.23758 (5)	0.511177 (20)
			Standard bracketing, data treatment: point by point PbP (95%)				
Average (n=6)	1.14005(35)	0.51130(3)	0.34871(5)	0.72310(20)	0.24232(15)	0.23783(52)	0.511177(26)

Table 3

References

1. J. G. Alonso, F. Sena, P. Arbore, M. Betti and L. Koch, *J. Anal. At. Spectrom.*, 1995, **10**, 381-393.
2. M. Betti, *J. Chromatogr., A*, 1997, **789**, 369-379.
3. F. Chartier, M. Aubert and M. Pilier, *Fres. J. Anal. Chem.*, 1999, **364**, 320-327.
4. A. Datta, N. Sivaraman, T. G. Srinivasan and P. R. Vasudeva Rao, *Nucl. Technol.*, 2013, **182**, 84-97.
5. P. Leconte, J.-F. Vidal, D. Bernard, A. Santamarina, R. Eschbach and J.-P. Hudelot, *Annals Nucl. Energy*, 2009, **36**, 362-367.
6. L. San-Felice, R. Eschbach and P. Bourdot, *Nucl. Technol.*, 2013, **184**, 217-232.
7. L. W. Green, C. H. Knight, T. H. Longhurst and R. M. Cassidy, *Anal. Chem.*, 1984, **56**, 696-700.
8. R. M. Cassidy, S. Elchuk, N. L. Elliot, L. W. Green, C. H. Knight and B. M. Recoskie, *Anal. Chem.*, 1986, **58**, 1181-1186.
9. C. H. Knight, R. M. Cassidy, B. M. Recoskie and L. W. Green, *Anal. Chem.*, 1984, **56**, 474-478.
10. A. Nonell, H. Isnard, M. Granet, J. Moureau, G. Favre and F. Chartier, in *ANIMMA International Conference*, Marseille, 2009.
11. M. Bourgeois, H. Isnard, A. Gourgiotis, G. Stadelmann, C. Gautier, S. Mialle, A. Nonell and F. Chartier, *J. Anal. At. Spectrom.*, 2011, **26**, 1549-1688.
12. W. Kerl, J. S. Becker, W. Dannecker and H. J. Dietze, *Fres. J. Anal. Chem.*, 1998, **362**, 433-439.
13. L. Perna, F. Bocci, L. A. d. l. Heras, J. D. Pablo and M. Betti, *J. Anal. At. Spectrom.*, 2002, **17**, 1166-1171.
14. S. Rollin, Z. Kopatjtic, B. Wernli and B. Magyar, *J. Chromatogr., A*, 1996, **739**, 139-149.
15. I. Günther-Leopold, N. Kivel, J. Kobler Waldis and B. Wernli, *Anal. Bioanal. Chem.*, 2008, **390**, 503-510.
16. J. A. Rodriguez-Castrillon, S. Garcia-Ruiz, M. Moldovan and J. I. Garcia Alonso, *J. Anal. At. Spectrom.*, 2012, **27**, 611-618.
17. M. Dzurko, D. Foucher and H. Hintelmann, *Anal. Bioanal. Chem.*, 2009, **393**, 345-355.
18. I. Günther-Leopold, B. Wernli, Z. Kopajtic and D. Günther, *Anal. Bioanal. Chem.*, 2004, **378**, 241-249.
19. E. Krupp, C. Pécheyran, S. Meffan-Main and O. X. Donard, *Anal. Bioanal. Chem.*, 2004, **378**, 250-255.
20. E. M. Krupp and O. F. X. Donard, *Int. J. Mass Spectrom.*, 2005, **242**, 233-242.
21. T. Pettke, F. Oberli, A. Audetat, U. Wiechert, C. R. Harris and C. A. Heinrich, *J. Anal. At. Spectrom.*, 2011, **26**, 475-492.
22. P. Rodríguez-González, V. N. Epov, C. Pecheyran, D. Amouroux and O. F. X. Donard, *Mass Spectrom. Rev.*, 2012, **31**, 504-521.
23. M. Tanner and D. Günther, *Anal. Chim. Acta*, 2009, **633**, 19-28.
24. H. Isnard, R. Brennetot, C. Caussignac, N. Caussignac and F. Chartier, *Int. J. Mass Spectrom.*, 2005, **246**, 66-73.
25. V. N. Epov, S. Berail, M. Jimenez-Moreno, V. Perrot, C. Pecheyran, D. Amouroux and O. F. X. Donard, *Anal. Chem.*, 2010, **82**, 5652-5662.
26. J. Fietzke, V. Liebetrau, D. Guenther, K. Gurs, K. Hametner, K. Zumholz, T. H. Hansteen and A. Eisenhauer, *J. Anal. At. Spectrom.*, 2008, **23**, 955-961.
27. T. Tanaka, S. Togashi, H. Kamioka, H. Amakawa, H. Kagami, T. Hamamoto, M. Yuhara, Y. Orihashi, S. Yoneda, H. Shimizu, T. Kunimaru, K. Takahashi, T. Yanagi, T. Nakano, H. Fujimaki, R. Shinjo, Y. Asahara, M. Tanimizu and C. Dragusanu, *Chem. Geol.*, 2000, **168**, 279-281.
28. J. C. Dubois, G. Retali and J. Cesario, *Int. J. Mass Spectrom. Ion Processes*, 1992, **120**, 163-177.
29. S. Wakaki and T. Tanaka, *Int. J. Mass Spectrom.*, 2012, **323–324**, 45-54.
30. W. A. Russell, D. A. Papanastassiou and T. A. Tombrello, *Geochim. Cosmochim. Acta*, 1978, **42**, 1075-1090.

31. A. Gourgiotis, S. Berail, P. Louvat, H. Isnard, J. Moureau, A. Nonell, G. Manhes, J.-L. Birck, J. Gaillardet, C. Pecheyran, F. Chartier and O. F. X. Donard, *J. Anal. At. Spectrom.*, 2014, **29**, 1607-1617.
32. L. Vio, G. Cretier, F. Chartier, V. Geertsen, A. Gourgiotis, H. Isnard, P. Morin and J. L. Rocca, *J. Anal. At. Spectrom.*, 2012, **27**, 850-856.
33. T. Ohno and T. Hirata, *Analyt. Sci.*, 2013, **29**, 47-53.
34. J. Chen, M. Nomura, Y. Fujii, F. Kawakami and M. Okamoto, *J. Nucl. Sci. Technol.*, 1992, **29**, 1086-1092.
35. I. M. Ismail, A. Fukami, M. Nomura and Y. Fujii, *Anal. Chem.*, 2000, **72**, 2841-2845.
36. I. M. Ismail, M. Ibrahim, H. F. Aly, M. Nomura and Y. Fujii, *J. Chromatogr., A*, 2011, **1218**, 2923-2928.
37. I. M. Ismail, M. Nomura and Y. Fujii, *J. Chromatogr., A*, 1998, **808**, 185-191.
38. Y.-H. Zhang, S. Gunji, M. Nomura, Y. Fujii and T. Oi, *J. Chromatogr., A*, 2005, **1069**, 133-139.
39. Y.-H. Zhang, M. Nomura, Y. Fujii and T. Oi, *Isot. Environm. Health Studies*, 2006, **42**, 279-288.
40. E. D. Young, A. Galy and H. Nagahara, *Geochim. Cosmochim. Acta*, 2002, **66**, 1095-1104.
41. J. R. Torres-Lapasió, J. J. Baeza-Baeza and M. C. García-Alvarez-Coque, *Anal. Chem.*, 1997, **69**, 3822-3831.
42. A. Gourgiotis, M. Granet, H. Isnard, A. Nonell, C. Gautier, G. Stadelmann, M. Aubert, D. Durand, S. Legand and F. Chartier, *J. Anal. At. Spectrom.*, 2010, **25**, 1939-1945.
43. H. Isnard, S. Eymard, G. Ferlay, P. Leveque, O. Vigneau and M. Phelip, International Conference on Fast Reactors ans Related Fuel Cycles: Safe Technologies and Sustainable Scenarios (FR13), Paris, 2013.
44. J. Tommasi, E. Dupont and P. Marimbeau, *Nucl. Sci. Eng.*, 2006, **154**, 119-133.
45. J. Tommasi and G. Nogurere, *Nucl. Sci. Eng.*, 2008, **160**, 232-241.
46. F. Goutelard, C. Caussignac, R. Brennetot, G. Stadelmann and C. Gautier, *J. Radioanal. Nucl. Chem.*, 2009, **282**, 669-675.
47. G. J. Wasserburg, S. B. Jacobsen, D. J. De Paolo, M. T. McCulloch and T. Wen, *Geochim. Cosmochim. Acta*, 1981, **45**, 2311-2323.
48. F. Albarède, P. Telouk, J. Blichert-Toft, M. Boyet, A. Agranier and B. Nelson, *Geochim. Cosmochim. Acta*, 2004, **68**, 2725-2744.
49. V. N. Epov, P. Rodriguez-Gonzalez, J. E. Sonke, E. Tessier, D. Amouroux, L. M. Bourgoin and O. F. X. Donard, *Anal. Chem.*, 2008, **80**, 3530-3538.
50. S. Mialle, Ph.D. Thesis, University Paul Sabatier Toulouse 3, 2011.

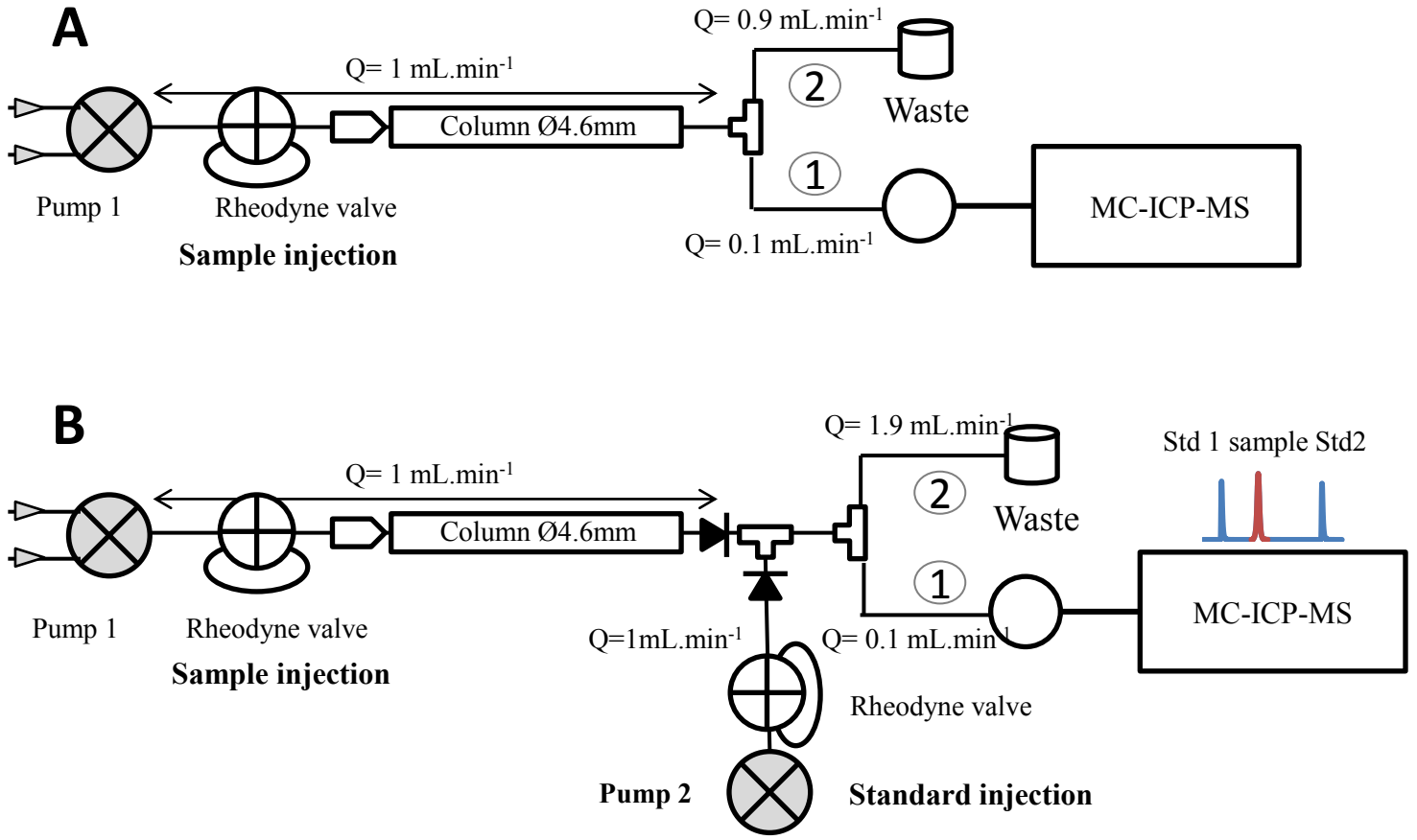

Figure 1: Schematic diagrams of (a) the LC-MC-ICPMS system and (b) the dual inlet LC-MC-ICPMS system with post-column addition of standard to perform intra injection mass bias correction.

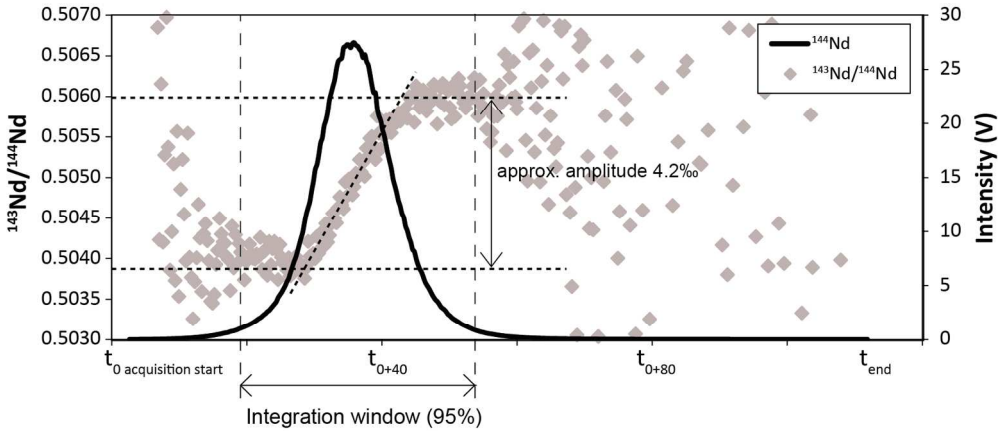

Figure 2: Elution profile of the 144Nd signal (JNdi-1 standard solution) by LC-MC-ICPMS in gradient mode (integration time 0.262 s) and uncorrected 143Nd/144Nd isotope ratios across the transient signals. The approximate amplitude of the drift was estimated by the variation of isotope ratios between the two horizontal lines.

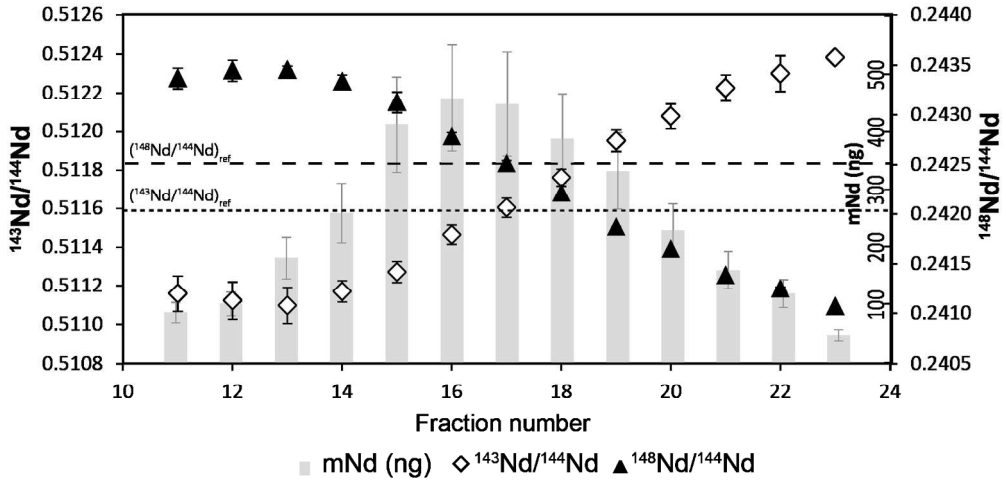

Figure 3: Nd concentration profile and 143Nd/144Nd and 148Nd/144Nd isotope ratios in the eluted drops after chromatographic separation on the LUNA SCX column (l=250 mm). The error bars for mass concentration correspond to a relative standard deviation equal to 20%. The error bars for isotope ratio correspond to a relative standard deviation at k=2 of three replicate analyses. The dotted lines represent the 143Nd/144Nd and 148Nd/144Nd reference values29.

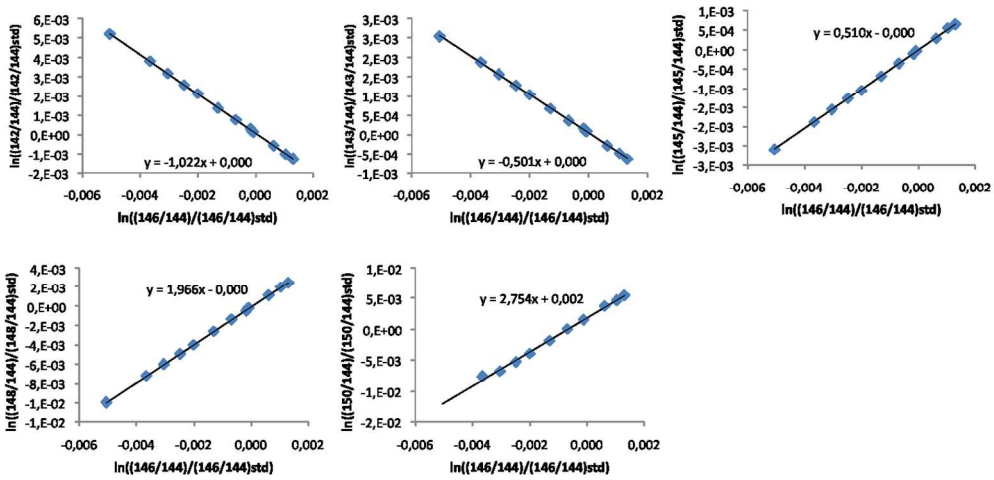

Figure 4: Three isotope plots of Nd isotope ratios using the approach developed by Young et al40. The experimental mass-dependent fractionation of the 14XNd/144Nd and 146Nd/144Nd was a straight line. The slope of the linear regression line was equal to the fractionation exponent β. The uncertainty associated with the Nd isotope ratios was smaller than the data points.

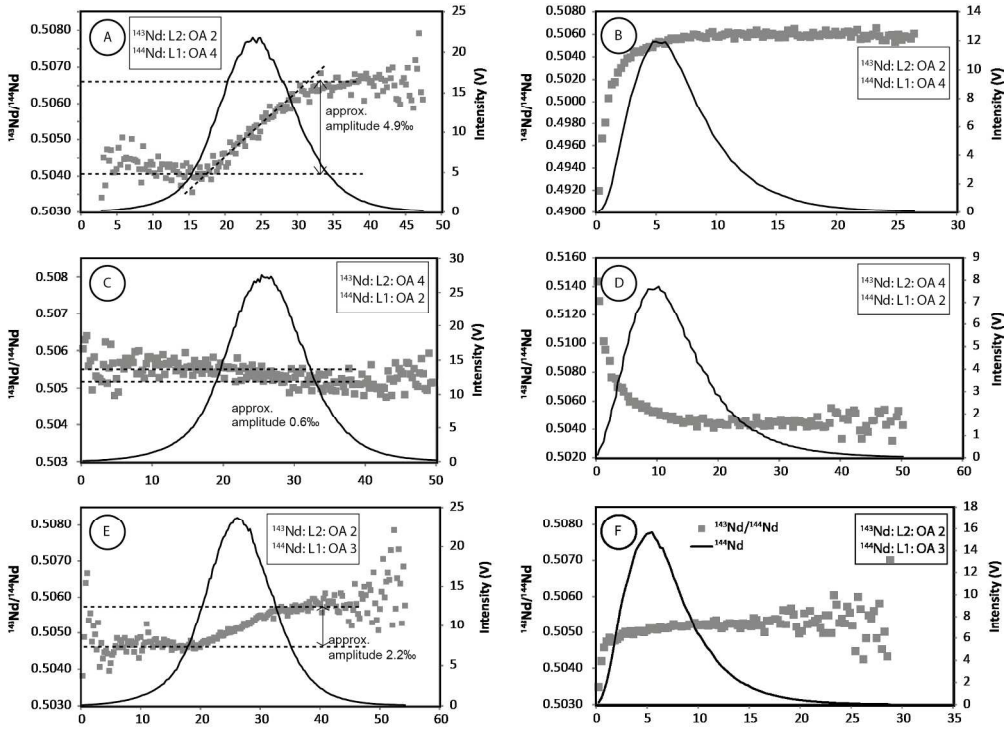

Figure 5: Uncorrected 143Nd/144Nd isotope ratio across the transient signals by LC-MC-ICPMS (A, C, E) and FIA (B, D, F). Different amplifiers were successively attributed to Faraday cups: configuration A and B: 143Nd: OA2; 144Nd OA 4; configuration C and D: 143Nd: OA 4; 144Nd OA 2; configuration E and F: 143Nd: OA2; 144Nd OA 3.

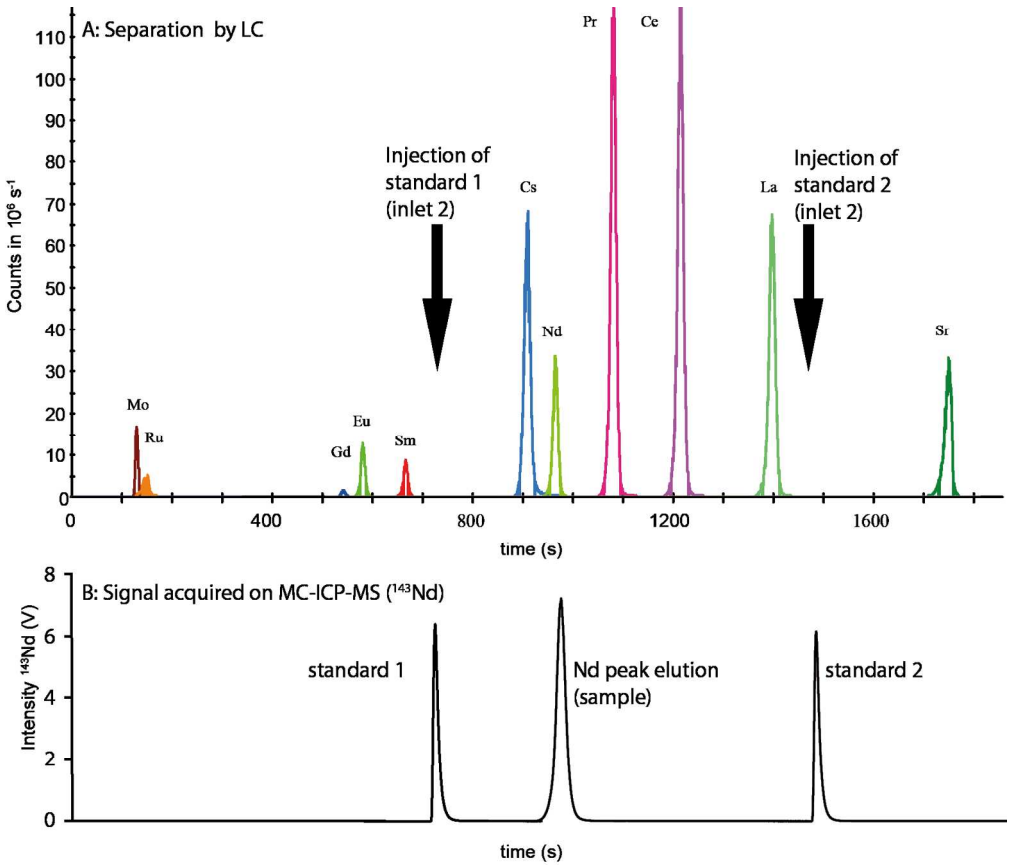

Figure 6: A: Chromatographic separation of a representative fission product fraction of a 235U-irradiated target with a LUNA SCX column (Ø 4.6 mm) at a flow rate of 1ml.min-1 and T=20°C. The elution gradient started at t=0 min with 100% HMB at 0.1M in water, pH=3.6 and finished at t=35min with 100% HMB at 0.2M in water, pH=4.5. B: 143Nd intensity signal recorded by MC-ICPMS during the time of elution. The Nd standard was injected between the Sm and Nd peaks (telution=720s) and after the La peak (telution=1450s).